Rotating optical vortex clusters in competing cubic-quintic media

Liangwei Dong [1,2,*] Guanqiang Li [1,2] and Changming Huang [3]
[1] Department of Physics, Shaanxi University of Science & Technology, Xi'an, 710021, China
[2] Institute of Theoretical Physics, Shaanxi University of Science & Technology, Xi'an, 710021, China
[3] Department of Electronic Information and Physics, Changzhi University, Changzhi, Shanxi, 046011, China

(Received 23 January 2022; accepted 20 April 2022; published 27 April 2022)

We put forward a rich variety of optical vortex structures nested in a localized beam envelope supported by cubic-quintic media confined in a rotating harmonic trap. The globally linked vortex cluster comprises an even number of vortices with topological charges equaling 1 and -1 alternately. In the nonrotating frame, single-charged vortices reside evenly on a ring. Yet, the system rotation induces the Coriolis force, which in turn leads to a strong asymmetry of the vortex cluster. With the increase of rotation frequency, vortex clusters with a different number of vortices transform into rotating nonlinear states with different symmetries. Meanwhile, the beam envelope is deformed obviously. Nonrotating vortex clusters are stable provided that their power exceeds a certain critical value. Unstable rotating states are very robust and survive over thousands of diffraction lengths.

DOI: 10.1103/PhysRevA.105.043522

I. INTRODUCTION

The generation, propagation, and interaction of vortices in nonlinear systems have been studied in diverse areas of physics, for example, nonlinear optics [1,2], Bose-Einstein condensates (BECs) [3], hydrodynamics, cavities, and electron beams [4], etc. Optical vortices are unique objects carrying a nonzero angular momentum expressed by a nontrivial phase distribution around a phase singularity [2]. They share many properties with the vortices observed in other systems, for instance, superfluids and BECs [5,6]. Applications of vortex solitons have been found in many fields, such as optical trapping, microscopy, and quantum information, etc., to name a few [7].

In Kerr or saturable nonlinear media, azimuthal symmetry-breaking instability usually breaks vortex soliton into several fragments. As has been revealed competing nonlinearity, such as a combination of $\chi^{(2)}$ and $\chi^{(3)}$ nonlinearity [8] and cubic-quintic [9] nonlinearity, can suppress the azimuthal instability effectively. Effective alternatives are confined systems, such as graded-index optical fibers [10], nonlinear photonic crystals with defects [11], linear and nonlinear optical lattices [12–15], and optical lattices with defects [16]. Experimentally, robust nonlinear vortex modes were observed in cubic-quintic and saturable media [17–19]. For a review of early works, see [2,20–22] and references therein.

Besides single vortex, vortex-antivortex pairs and quadrupoles nested in a localized beam field were reported [23,24]. However, only vortex-antivortex pairs can stably evolve in a narrow parameter region. Very different vortex solitons, rotating vortex clusters, were proposed in media with inhomogeneous defocusing nonlinearity whose strength grows to the periphery at a rate faster than r^D, where D is the dimension of space [25]. Rotating twin-vortex solitons [26] and vortex breathers [27] were discussed in nonlocal nonlinear media. Surface solitons can rotate stably at the edge of the guiding structures consisting of several concentric rings [28]. Truncated rotating square waveguide arrays support new types of localized modes in both linear and nonlinear cases [29]. Ultrashort light bullets were found in strongly twisted waveguide arrays [30]. Robust rotating azimuthons excited by superpositions of Bessel beams were studied in dissipative Kerr media [31]. The rotation may stabilize in somewhat unstable solitons.

In BECs, vortex clusters have been studied in parabolic traps [32–35]. Multisolitons and azimuthons were numerically solved by a numerical relaxation procedure with a stabilizing factor [34]. Stable three-dimensional nonrotating and rotating (azimuthon) multipole solitons were also obtained numerically by the same method [35]. Vortex replication was reported in BECs trapped in double-well potentials [36]. Metastable rotating vortex clusters were revealed in the form of quantum droplets carrying multiple singly quantized vortices held in a parabolic potential modeled by the Gross-Pitaevskii equation augmented with Lee-Huang-Yang corrections [37]. Very recently, we predicted an interesting type of two-dimensional and three-dimensional stable quantum droplets persistently rotating in an anharmonic potential. Through rotation, crescentlike droplets bridge fundamental droplets and vortex droplets with different topological charges [38].

Despite the above progress, the properties of rotating optical vortex clusters have not been explored in homogeneous nonlinear medium. The goal of this paper is to draw a full picture of the dynamics of rotating vortex clusters (rotating complex solitons) in optical media with a homogeneous nonlinearity. We investigate the existence, stability, and propagation dynamics of the rotating complex solitons, as well as the impact of the Coriolis force on their properties. Our

*dlw_0@163.com

prediction may provide a helpful hint for the experimental creation of elusive self-sustained complex vortex states in nonlinear optics and BECs.

II. THEORETICAL MODEL

Our analysis starts from considering light propagation along the z axis of a competing cubic-quintic medium. Dynamics of the beam in an external potential is governed by a two-dimensional nonlinear Schrödinger equation:

$$i\frac{\partial\Psi}{\partial z} = -\frac{1}{2}\left(\frac{\partial^2\Psi}{\partial x^2} + \frac{\partial^2\Psi}{\partial y^2}\right) + V\Psi - |\Psi|^2\Psi + |\Psi|^4\Psi, \quad (1)$$

where the scaling invariances of the system have been used to bring the equation into this dimensionless form. Potential $V(x, y) = \omega^2 r^2/2$ stands for a harmonic trapping with $r = \sqrt{x^2 + y^2}$ and ω being the trapping frequency. To find rotating vortex clusters, we use coordinate frame $[x' = x\cos(\Omega z) + y\sin(\Omega z), y' = y\cos(\Omega z) - x\sin(\Omega z)]$ that rotates around the z axis with a rotation frequency (angular velocity) Ω, where Eq. (1) acquires the following form:

$$i\frac{\partial\Psi}{\partial z} = \left[-\frac{1}{2}\left(\frac{\partial^2}{\partial x^2} + \frac{\partial^2}{\partial y^2}\right) + V - |\Psi|^2 + |\Psi|^4 - \Omega L_z\right]\Psi. \quad (2)$$

We omitted the primes in the rotating coordinate system Eq. (2). The Coriolis term induced by the rotation is expressed by $-\Omega L_z\Psi$ with $L_z = -i(x\partial/\partial y - y\partial/\partial x)$. The rotation frequency $\Omega > 0$ corresponds to the counterclockwise rotation. The beam evolution is characterized by the power (energy flow) $U = \iint |\Psi(x, y)|^2 dxdy$ and the angular momentum $L = \iint \Psi^* L_z \Psi dxdy$.

The stationary solution of Eq. (2) in the rotating frame can be solved by assuming $\Psi(x, y, z) = \psi(x, y)\exp(ibz)$, where b is a real propagation constant and $\psi = \psi_r + i\psi_i$ is the profile of a soliton with real part ψ_r and imaginary part ψ_i. The field modulus is defined as $|\psi| = \sqrt{\psi_r^2 + \psi_i^2}$ and the phase structure is determined by the relation $\theta = \arctan(\psi_i/\psi_r)$. Substitution of the expression into Eq. (2) yields a coupled partial differential equation, from which soliton solutions can be solved numerically by using the Newton-conjugate gradient method [39]. The basic idea is to use Newton iterations, coupled with conjugate-gradient iterations to solve the resulting linear Newton-correction equation. It can converge for both the nonlinear ground states and excited states. Typical examples show that the Newton-conjugate gradient method converges much faster than the other existing iteration methods, often by orders of magnitude. For details of this numerical method, see pages 381–389 in Ref. [39].

Since single-charged vortex solitons in cubic-quintic media are stable only for $b \in [0.145, 0.1813]$ [40,41], we introduce a weakly harmonic potential to extend the stability region. The external potential enlarges the existence domain of vortices simultaneously. For the sake of definiteness and illustration, we set $\omega = 0.02$ throughout this paper. The nonlinear mode in the absence of an external potential has a characteristic flat-top shape when its power is relatively large. The trapping frequency is sufficiently weak to keep the nonlinear state at a power close to its (free) equilibrium value. Meanwhile, the harmonic potential confines the light field around its center,

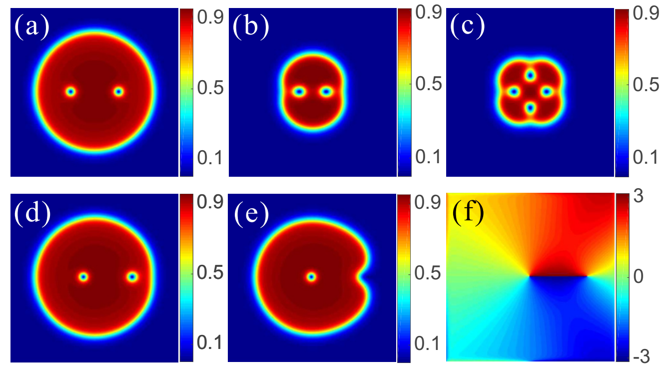

FIG. 1. (a) and (b) Field moduli of nonrotating vortex dipoles at $b = 0.0643$ and $b_{\text{cut}} = 0.1307$, respectively. (c) Nonrotating vortex quadrupole at $b_{\text{cut}} = 0.1267$. (d) and (e) Rotating vortex dipoles at $\Omega = 0.002$ and 0.0095, respectively. (f) Phase distribution corresponding to (e). $b = 0.0643$ in (d) and (f), $U = 1500$ in (a), and $x, y \in [-35, 35]$ in all the panels.

which makes it possible to form vortex clusters. Indeed, in a system without an external potential, one cannot find nonlinear modes containing vortices with pivot positions deviating from the center of the field envelope.

To obtain the stationary solutions of vortex clusters, we guess the initial nonlinear modes in the form,

$$\psi(x, y) = A\exp(-r^4/w^4)\sum_{k=1}^{n}\exp\left[i(-1)^k \arctan\frac{y - y_k}{x - x_k}\right], \quad (3)$$

where $A\exp(-r^4/w^4)$ is a super-Gaussian background light field, the even integer n is the total number of single-charged vortices, k is a sequence number, $(-1)^k$ denotes the topological charge of vortices with alternate signs for the neighboring vortices, $x_k = r_0\cos(\theta_k)$ and $y_k = r_0\sin(\theta_k)$ $[\theta_k = 2(k-1)\pi/n]$ are the positions of vortex pivots, r_0 is the radius of a ring on which the centers of vortices reside, and $\phi_k = \arctan\frac{y-y_k}{x-x_k}$ is the angular coordinates around the vortex pivots at (x_k, y_k).

III. NUMERICAL RESULTS AND DISCUSSION

Before unveiling the vortex clusters containing multiple single-charged vortices, it is beneficial to understand the properties of vortex dipoles first. In the nonrotating regime ($\Omega = 0$), a vortex dipole contains two vortices with opposite topological charges ($m_1 = -m_2 = 1$) residing symmetrically with respect to the origin at $x, y = 0$ [Fig. 1(a)]. With the growth of propagation constant b, the right vortex moves toward the origin (the left one is always symmetric with the right one). As b approaches its upper cutoff $b_{\text{cut}} = 0.1307$, though the twin vortices are still symmetric about the origin, the beam envelope shrinks and becomes deformed obviously [Fig. 1(b)]. Concretely, it is squeezed along two mutually perpendicular directions with different rates, which makes the envelope no longer radially symmetric, in sharp contrast to vortex dipoles in inhomogeneous defocusing media [25].

The Coriolis force emerges when the system rotates around the z axis. It plays an important role in the motion of vortices. The opposite winding numbers of the neighboring vortices

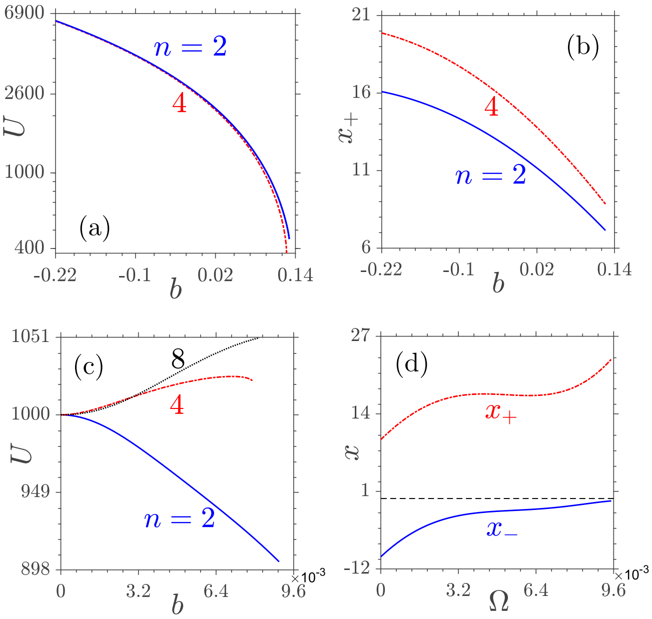

FIG. 2. (a) Dependence of power U on b for nonrotating vortex dipoles and quadrupoles. (b) Variation of positions of the vortex pivots versus b for nonrotating vortex dipoles and quadrupoles. (c) $U(\Omega)$ curves for rotating vortex dipoles at $b = 0.0973$ (solid), quadrupoles at $b = 0.0934$ (dash-dotted), and octopoles at $b = 0.0868$ (dotted); $U(\Omega = 0) = 1000$ for all curves. (d) Variation of positions of the vortex pivots versus Ω for rotating vortex dipoles at $b = 0.0643$, $U(\Omega = 0) = 1500$. Dashed line denotes $x = 0$.

indicate that the directions of the azimuthally internal currents of neighboring embedded vortices are opposite. When Ω is fixed, the Coriolis force "felt" by $m = 1$ vortices is different from that "felt" by $m = -1$ vortices. For instance, the rotation makes the left vortex ($m = -1$) in the vortex dipole move toward the origin and the right vortex ($m = 1$) move toward the periphery [Figs. 1(d) and 1(e)]. Thus, the Coriolis force induced by the rotation destroys the symmetry of $m = \pm 1$ vortices at $\Omega = 0$ [Fig. 1(a)]. In this process, the distance between two vortices varies slightly. At $\Omega_{\text{cut}} = 0.0095$, even if we neglect the sign of m, the phase of the right vortex is still not symmetric with that of the left one [Fig. 1(f)].

The power of nonrotating vortex dipoles decreases with b [Fig. 2(a)]. The nonzero threshold power at $b_{\text{cut}} = 0.1307$ implies that such modes are purely nonlinear states and cannot bifurcate out from the eigenmodes of the corresponding linear system. As b decreases, the beam envelope expands and a giant flat-top beam with nested vortices forms at high power [Fig. 1(a)]. The distance between the two vortices in the nonrotating vortex dipole decreases monotonically with the growth of b [Fig. 2(b)].

The power of vortex dipoles at fixed b decreases monotonically with the growth of Ω [Fig. 2(c)]. There is a cutoff value Ω_{cut} above which no stationary solutions of rotating vortex dipoles can be found [see, e.g., Figs. 2(c) and 4(d)]. At Ω_{cut}, the left vortex reaches the origin and the right one moves outside of the beam envelope [Fig. 1(e)]. Unlike the right vortex in Fig. 1(e) at Ω_{cut}, the two vortices in the nonrotating

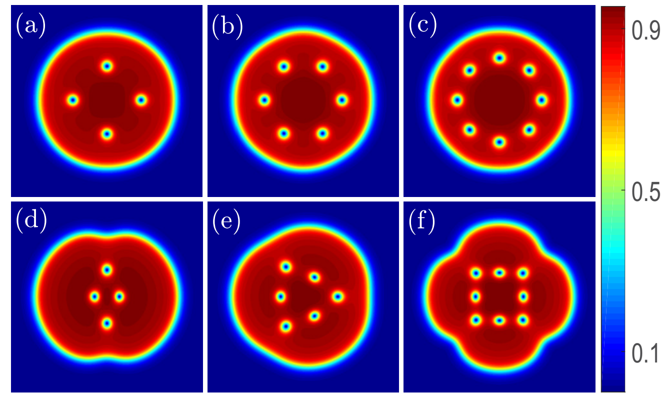

FIG. 3. Field moduli of vortex clusters. (a) and (d) Vortex quadrupoles at $b = 0.0611$. (b) and (e) Vortex sextupoles at $b = 0.0584$. (c) and (f) Vortex octopoles at $b = 0.0560$. $\Omega = 0.0089$, 0.0066, and 0.002 in (d),(e), and (f), respectively. $\Omega = 0$, $U = 1500$ in (a)–(c) and $x, y \in [-35, 35]$ in all the panels.

vortex dipole at b_{cut} are still surrounded by the beam envelope [Fig. 1(b)].

Of particular interest is the process of the variation of the positions of vortex pivots versus rotation frequency [Fig. 2(d)]. When Ω is below 0.0038, the two vortices move rapidly toward positive infinity and the distance between them is invariant. While the right vortex resides on a fixed position $x_+ \approx 17.2$ in the region $\Omega \in [0.0038, 0.0066]$, the left vortex still moves slowly toward the origin. For $\Omega > 0.0066$, the linear velocity of the right vortex is faster than that of the

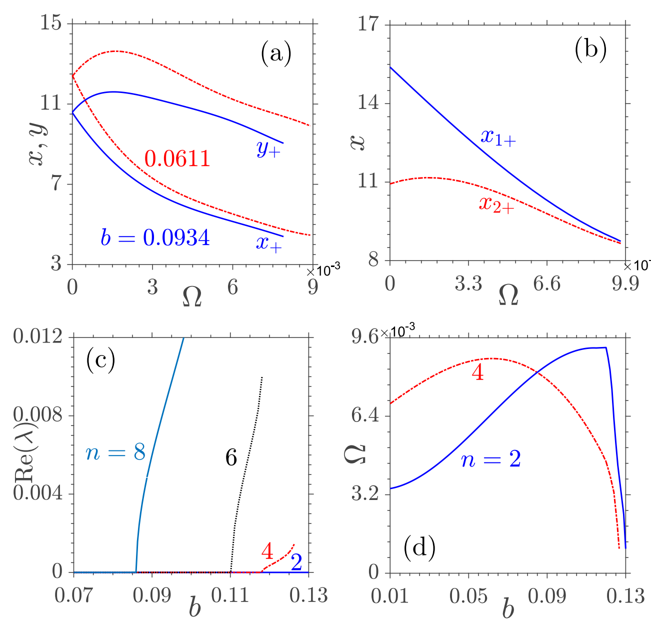

FIG. 4. The variation of the positions of the vortex pivots versus Ω for vortex quadrupoles (a) and octopoles (b). $U(\Omega = 0) = 1500$ and 1000 is shown in (a). The x_+, y_+ in (a) denote the position of the right and upper vortices. The x_{1+}, x_{2+} in (b) represent the positions of the right and upper-right vortices. (c) Instability growth rate $\mathrm{Re}(\lambda)$ versus b for nonrotating vortex clusters. (d) Existence domains of vortex dipoles and quadrupoles on the $(b - \Omega)$ plane.

left vortex. Eventually, the left vortex approaches the origin and the right one reaches the edge of the beam envelope. The unequal linear velocities of the two vortices and the nonuniformly linear velocities of a single vortex may be related to the nonlinear variation of vortex dipole power on the rotation frequency Ω [Fig. 2(c)].

The symmetry of vortex clusters containing more vortices can be analyzed by the group theory briefly. The rotational symmetry of nonlinear modes is usually determined by the form of the external potential [42]. The harmonic potential adopted here shows perfect continuous rotational symmetry since $V(r)$ has no dependence on the azimuth angle ϕ. The symmetry group of $V(r)$ is thus $\mathcal{O}(2)$ and has no influence on the symmetry of nonlinear states. Yet, considering the fact that an even number of vortices with alternating winding numbers resides on a ring, the rotational symmetry group of vortex clusters containing n vortices is determined by the discrete point-symmetry group $\mathcal{C}_{n/2,v}$. This corresponds to discrete rotations of the azimuth angle $\epsilon_n = 4\pi/n$ with respect to a rotation axis perpendicular to the (x, y) plane and intersecting it at the origin as well as to specular reflections with respect to a number of planes containing the rotation axis [43]. The relation $\psi(r, \phi + \epsilon_n) = \psi(r, \phi)$ holds for both nonrotating and rotating vortex clusters containing an even number of vortices (Fig. 3).

The variation of positions of vortex pivots and the distribution of the field envelope in nonrotating vortex clusters containing more vortices are similar to those of vortex dipoles. For vortex quadrupoles at $\Omega = 0$, four vortices with alternating charges reside evenly on a ring [Fig. 3(a)]. The beam envelope exhibits a radial symmetry when b is small. Yet, as b approaches to $b_{\text{cut}} = 0.1267$, the field envelope of the vortex quadrupole is squeezed along two mutually perpendicular directions at the same rate. The shrinkage makes the envelope no longer radially symmetric and it becomes a squarelike one [Fig. 1(c)]. Similarly, when $b \to b_{\text{cut}}$, the envelopes of the vortex sextupole and octopole become a regular hexagon and a regular octagon, respectively. This is in sharp contrast to the vortex quadrupole and sextupole in inhomogeneous nonlinearity [25], where the beam envelope is always radially symmetric.

Unlike the vortex dipole, the counterclockwise rotation ($\Omega > 0$) of the vortex quadrupole results in the four vortices moving toward the origin. The $m = -1$ vortices on the y axis move slower than the $m = 1$ vortices on the x axis [Figs. 3(a) and 3(d)]. The vortex quadrupole at $\Omega = -0.0089$ can be obtained by rotating the vortex quadrupole at $\Omega = 0.0089$ shown in Fig. 3(d) by $\pi/2$. It manifests the fact that the effect of counterclockwise rotation on $m = \mp 1$ vortices is the same as that of the clockwise rotation on $m = \pm 1$ vortices.

The rearrangement of vortices due to rotation changes the symmetry of the field envelope simultaneously. While rotating vortex quadrupoles remain symmetric about the x and y axes [Figs. 3(d)], rotating vortex sextupoles are only symmetric about the x axis [Fig. 3(e)]. Near Ω_{cut}, the vortices reside in a regular triangle for vortex sextupoles and a regular square for vortex octopoles [Fig. 3(f)]. The envelope is deformed more severely near the corners of the regular polygons. This property provides a possibility for the realization of beam reshaping in a rotating regime by appropriately placing different numbers of single-charged vortices in a flat-top beam.

In vortex quadrupoles, while the vortices on the x axis move to the origin with the growth of Ω, the vortices on the y axis move toward the periphery first and turn back to the origin when the rotational frequency exceeds a certain value Ω_{cr} [Fig. 4(a)]. For $\Omega > \Omega_{\text{cr}}$, the moving speed of vortices on the x axis is the same as that of the vortices on the y axis. Given the symmetry of vortex octopoles, one only needs to monitor the variation of positions of the right vortex and upper-right vortex [Fig. 4(b)]. While the right vortex holds a uniform motion toward the origin, the upper-right vortex is almost static at small Ω and moves along a 45% direction for large Ω.

The stability of rotating vortex clusters can be analyzed by solving the perturbed solutions of Eq. (2) in the form $\Psi(x, y, z) = [\psi(x, y) + u(x, y)\exp(\lambda z) + v^*(x, y)\exp(\lambda^* z)]\exp(ibz)$, where u and $v \ll 1$ are infinitesimal perturbations and λ is the growth rate of the instability. Linearization of Eq. (2) around stationary solutions yields an eigenvalue problem [44]:

$$i\begin{bmatrix} \mathcal{M}_1 & \mathcal{M}_2 \\ -\mathcal{M}_2^* & -\mathcal{M}_1^* \end{bmatrix}\begin{bmatrix} u \\ v \end{bmatrix} = \lambda \begin{bmatrix} u \\ v \end{bmatrix}, \tag{4}$$

where $\mathcal{M}_1 = (\partial^2/\partial x^2 + \partial^2/\partial y^2)/2 - \omega^2(x^2 + y^2)/2 - b + 2|\psi|^2 - 3|\psi|^4 - i\Omega(x\partial/\partial y - y\partial/\partial x)$, $\mathcal{M}_2 = \psi^2(1 - 2|\psi|^2)$, and $*$ denotes complex conjugate. The instability growth rate λ in Eq. (4) was solved numerically using a Fourier collocation method [39]. Solitons are stable only when all *positive* real parts of the eigenvalues λ equal zero.

Figure 4(c) shows the dependence of the instability growth rate on propagation constant b for nonrotating vortex clusters. Vortex dipoles are completely stable. Vortex clusters with $n \geqslant 4$ are stable provided that the condition $b < b_{\text{cr}}$ or $U > U_{\text{cr}}$ is satisfied. The stability region shrinks with the growth of the number of vortices n.

However, with the increase of Ω, a weak instability occurs for vortex clusters containing four or more vortices, which may be linked with the dependence of power on Ω [Fig. 2(c)]. While the power of vortex dipoles decreases with Ω, the power of vortex clusters with more vortices increases. The principle of minimum energy implies that the rotating state with increasing power suffers instability. Strictly speaking, rotating vortex clusters with four or more vortices are unstable. Nevertheless, the instability growth rate is very small and grows very slowly with Ω, which allows vortex clusters to survive for a very long propagation distance. This indicates that even unstable rotating states can be seen as stable objects in practice, as we will show in Fig. 5. The allowed maximal Ω for vortex dipoles increases slowly with the growth of b first and drops down abruptly when $b > 0.12$. The largest Ω_{cut} of vortex quadrupoles appears at moderate power [Fig. 4(d)].

The stability analysis results are verified by exhaustively numerical propagation simulations of Eq. (1) using split-step Fourier algorithm. Typical examples are shown in Fig. 5. Rotating vortex dipoles are completely stable in their entire existence domain. All vortex clusters rotate counterclockwise when $\Omega > 0$. The rotational periodicity of vortex clusters estimated by the relation $T = 2\pi/\Omega$ precisely predicts the

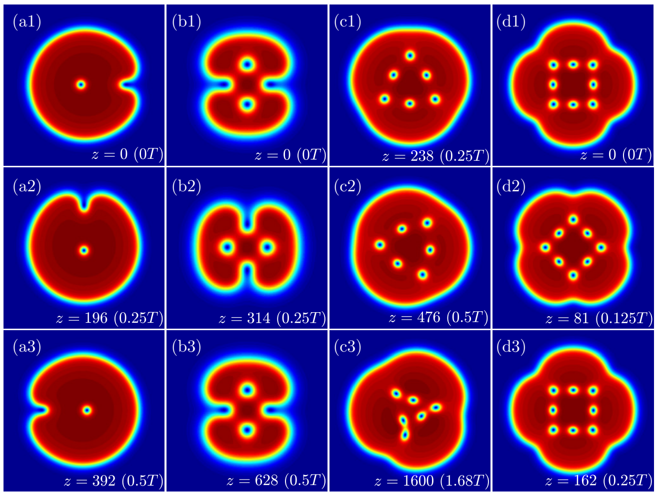

FIG. 5. Stable (a) and unstable (b)–(d) propagation examples of vortex clusters. $b = 0.0643$, $\Omega = 0.008$ in (a), $b = 0.12$, $\Omega = 0.005$ in (b), $b = 0.0584$, $\Omega = 0.0066$ in (c), $b = 0.0560$, $\Omega = 0.0097$ in (d). $(x, y) \in [-35, 35]$ in (a), (c), (d) and $[-25, 25]$ in (b).

propagation dynamics of the rotating vortex clusters. For example, the periodicity for vortex quadrupoles with $\Omega = 0.005$ shown in Fig. 5(b) is $\sim$1256. The initial input of Fig. 5(c) is shown in Fig. 3(e). The vortices in the vortex sextupole begin to merge at $z = 1600$. Though vortex clusters are unstable in certain parameter ranges of b and Ω, their instability growth rates are very small which allows them to survive for a very long distance (thousands of diffraction lengths), greatly exceeding the present experimentally feasible sample lengths. Such unstable nonlinear states can be regarded as dynamically stable objects.

IV. CONCLUSIONS

In summary, we studied the propagation dynamics of rotating vortex clusters in a system modeled by the nonlinear Schrödinger equation with a cubic-quintic nonlinearity and a harmonic trapping potential. Various families of stationary solutions, including vortex dipoles, quadrupoles, sextupoles, and octopoles were derived in nonrotating and rotating regimes. For nonrotating modes, while vortices keep their symmetry with the decrease of propagation constant, the envelope loses its radial symmetry as $b \to b_{\text{cut}}$. For vortex clusters with a radially symmetric envelope, the increase of Ω shifts the positions of vortices and destroys the symmetry of both the envelope and the vortices. Nonrotating vortex clusters are stable in a very broad region. The unstable rotating states can survive over a very long propagation distance without obvious deformations. The findings can be generalized to the investigation of vortex clusters in media with $\chi^{(2)} - \chi^{(3)}$ nonlinearity modulated by parabolic or other radially symmetric potentials. In addition, our results are relevant for matter-wave solitons or quantum droplets trapped in a harmonic potential.

ACKNOWLEDGMENTS

This work is supported by the Natural Science Basic Research Program in Shaanxi Province of China (Grants No. 2022JZ-02 and No. 2020JM-507).

[1] Y. S. Kivshar and G. P. Agrawal, *Optical Solitons: From Fibers to Photonic Crystals* (Academic, San Diego, 2003).

[2] A. S. Desyatnikov, Y. S. Kivshar, and L. Torner, Optical vortices and vortex solitons, Prog. Opt. **47**, 291 (2005).

[3] S. Donadello, S. Serafini, M. Tylutki, L. P. Pitaevskii, F. Dalfovo, G. Lamporesi, and G. Ferrari, Observation of Solitonic Vortices in Bose-Einstein Condensates, Phys. Rev. Lett. **113**, 065302 (2014).

[4] L. M. Pismen, *Vortices in Nonlinear Fields: From Liquid Crystals to Superfluids, From Non-equilibrium Patterns to Cosmic Strings* (Clarendon Press, Oxford, 1999).

[5] K. W. Madison, F. Chevy, W. Wohlleben, and J. Dalibard, Vortex Formation in a Stirred Bose-Einstein Condensate, Phys. Rev. Lett. **84**, 806 (2000).

[6] C. Raman, J. Abo-Shaeer, J. Vogels, K. Xu, and W. Ketterle, Vortex Nucleation in a Stirred Bose-Einstein Condensate, Phys. Rev. Lett. **87**, 210402 (2001).

[7] J. P. Torres and L. Torner, *Twisted Photons: Application of Light with Orbital Angular Momentum* (Wiley-VCH, Weinheim, 2011).

[8] D. Mihalache, D. Mazilu, L.-C. Crasovan, I. Towers, B. A. Malomed, A. V. Buryak, L. Torner, and F. Lederer, Stable three-dimensional spinning optical solitons supported by competing quadratic and cubic nonlinearities, Phys. Rev. E **66**, 016613 (2002).

[9] M. Quiroga-Teixeiro and H. Michinel, Stable azimuthal stationary state in quintic nonlinear optical media, J. Opt. Soc. Am. B **14**, 2004 (1997).

[10] S. Raghavan and G. P. Agrawal, Spatiotemporal solitons in inhomogeneous nonlinear media, Opt. Commun. **180**, 377 (2000).

[11] A. Ferrando, M. Zacarés, P. Fernández de Córdoba, D. Binosi, and J. A. Monsoriu, Vortex solitons in photonic crystal fibers, Opt. Express **12**, 817 (2004).

[12] J. Yang and Z. H. Musslimani, Fundamental and vortex solitons in a two-dimensional optical lattice, Opt. Lett. **28**, 2094 (2003).

[13] B. B. Baizakov, B. A. Malomed and M. Salerno, Multidimensional solitons in periodic potentials, Europhys. Lett. **63**, 642 (2003).

[14] Y. V. Kartashov, V. A. Vysloukh, and L. Torner, Stable Ring-Profile Vortex Solitons in Bessel Optical Lattices, Phys. Rev. Lett. **94**, 043902 (2005).

[15] N. Dror and B. A. Malomed, Solitons and vortices in nonlinear potential wells, J. Opt. **18**, 014003 (2016).

[16] L. Dong and F. Ye, Shaping solitons by lattice defects, Phys. Rev. A **82**, 053829 (2010).

[17] A. S. Reyna and C. B. D. Araújo, Guiding and confinement of light induced by optical vortex solitons in a cubic–quintic medium, Opt. Lett. **41**, 191 (2016).

[18] A. S. Reyna, G. Boudebs, B. A. Malomed, and C. B. D. Araújo, Robust self-trapping of vortex beams in a saturable optical medium, Phys. Rev. A **93**, 013840 (2016).

[19] A. S. Reyna, H. T. M. C. M. Baltar, E. Bergmann, A. M. Amaral, E. L. Falcão-Filho, P.-F. Brevet, B. A. Malomed, and C. B. D. Araújo, Observation and analysis of creation, decay, and regeneration of annular soliton clusters in a lossy cubic-quintic optical medium, Phys. Rev. A **102**, 033523 (2020).
[20] F. Lederer, G. I. Stegeman, D. N. Christodoulides, G. Assanto, M. Segev, and Y. Silberberg, Discrete solitons in optics, Phys. Rep. **463**, 1 (2008).
[21] Y. V. Kartashov, V. A. Vysloukh, and L. Torner, Soliton shape and mobility control in optical lattices, Prog. Opt. **52**, 63 (2009).
[22] B. A. Malomed, (INVITED) Vortex solitons: Old results and new perspectives, Physica D **399**, 108 (2019).
[23] R. Driben, N. Dror, B. A. Malomed, and T. Meier, Multipoles and vortex multiplets in multidimensional media with inhomogeneous defocusing nonlinearity, New J. Phys. **17**, 083043 (2015).
[24] D. Feijoo, A. Paredes, and H. Michinel, Dynamics of vortex-antivortex pairs and rarefaction pulses in liquid light, Phys. Rev. E **95**, 032208 (2017).
[25] Y. V. Kartashov, B. A. Malomed, V. A. Vysloukh, M. R. Belić, and L. Torner, Rotating vortex clusters in media with inhomogeneous defocusing nonlinearity, Opt. Lett. **42**, 446 (2017).
[26] F. Ye, Y. V. Kartashov, B. Hu, and L. Torner, Twin-vortex solitons in nonlocal nonlinear media, Opt. Lett. **35**, 628 (2010).
[27] Y. Chen and G. Liang, Rotating vortex clusters nested in Gaussian envelope in nonlocal nonlinear media, Opt. Commun. **449**, 69 (2019).
[28] Y. V. Kartashov, V. A. Vysloukh, and L. Torner, Rotating surface solitons, Opt. Lett. **32**, 2948 (2007).
[29] X. Zhang, F. Ye, Y. V. Kartashov, V. A. Vysloukh, and X. Chen, Localized waves supported by the rotating waveguide array, Opt. Lett. **41**, 4106 (2016).
[30] C. Milián, Y. V. Kartashov, and L. Torner, Robust Ultrashort Light Bullets in Strongly Twisted Waveguide Arrays, Phys. Rev. Lett. **123**, 133902 (2019).
[31] C. Ruiz-Jiménez, H. Leblond, M. A. Porras, and B. A. Malomed, Rotating azimuthons in dissipative Kerr media excited by superpositions of Bessel beams, Phys. Rev. A **102**, 063502 (2020).
[32] L.-C. Crasovan, G. Molina-Terriza, J. P. Torres, L. Torner, V. M. Pérez-García, and D. Mihalache, Globally linked vortex clusters in trapped wave fields, Phys. Rev. E **66**, 036612 (2002).
[33] V. M. Lashkin, A. S. Desyatnikov, E. A. Ostrovskaya, and Y. S. Kivshar, Azimuthal vortex clusters in Bose-Einstein condensates, Phys. Rev. A **85**, 013620 (2012).
[34] V. M. Lashkin, Two-dimensional multisolitons and azimuthons in Bose-Einstein condensates, Phys. Rev. A **77**, 025602 (2008).
[35] V. M. Lashkin, Stable three-dimensional spatially modulated vortex solitons in Bose-Einstein condensates, Phys. Rev. A **78**, 033603 (2008).
[36] J. R. Salgueiro, M. Zacarés, H. Michinel, and A. Ferrando, Vortex replication in Bose-Einstein condensates trapped in double-well potentials, Phys. Rev. A **79**, 033625 (2009).
[37] M. N. Tengstrand, P. Stürmer, E. O. Karabulut, and S. M. Reimann, Rotating Binary Bose-Einstein Condensates and Vortex Clusters in Quantum Droplets, Phys. Rev. Lett. **123**, 160405 (2019).
[38] L. Dong and Y. V. Kartashov, Rotating Multidimensional Quantum Droplets, Phys. Rev. Lett. **126**, 244101 (2021).
[39] J. Yang, *Nonlinear Waves in Integrable and Nonintegrable Systems* (SIAM, Philadelphia, 2010).
[40] I. Towers, A. V. Buryak, R. A. Sammut, B. A. Malomed, L.-C. Crasovan, and D. Mihalache, Stability of spinning ring solitons of the cubic-quintic nonlinear Schrödinger equation, Phys. Lett. A **288**, 292 (2001).
[41] L. Dong, F. Ye, J. Wang, T. Cai, and Y.-P. Li, Internal modes of localized optical vortex soliton in a cubic-quintic nonlinear medium, Physica D **194**, 219 (2004).
[42] Y. V. Kartashov, A. Ferrando, A. A. Egorov, and L. Torner, Soliton Topology versus Discrete Symmetry in Optical Lattices, Phys. Rev. Lett. **95**, 123902 (2005).
[43] M. Hamermesh, *Group Theory and Its Application to Physical Problems, Addison-Wesley Series in Physics* (Addison-Wesley, Reading, 1964).
[44] J. Yang, Partially PT symmetric optical potentials with all-real spectra and soliton families in multidimensions, Opt. Lett. **39**, 1133 (2014).